

# Influence of additives on the morphological, phase and chemical characteristics of gas sensitive SnO<sub>2</sub> sprayed films

I. STAMBOLOVA, K. KONSTANTINOV

*BAS, Institute of General and Inorganic Chemistry, Acad. G. Bonchev Blvd., Bl. 11, 1113 Sofia, Bulgaria*

The morphology, and also the chemical and phase composition of sprayed SnO<sub>2</sub> films doped with Cu, Zr, Fe and P have been investigated. It was found that in general, the film morphology was characterized by a fine grained basic layer with a few large crystallites located on the surface. All the doping elements decreased the grain size in the basic layer. For Fe, Zr and P the grain size depended on the doping level in the spray solution. It was established that the dopant:Sn ratio in the films was much lower than that in the spray solution. The doping element was preferentially accommodated in the large crystallites with only a small quantity of the dopant being introduced into the basic layer. The gas sensing properties of the films have are discussed on the basis of these results.

## 1. Introduction

Thin films of SnO<sub>2</sub> find application in gas sensors, photovoltaic and optoelectronic elements and many other electronic devices. It is known that charge transport across grain boundaries is responsible for the gas sensitivity of these films [1]. Therefore, the microstructure of the films is one of the basic factors that determines the gas sensitivity. Currently, the addition of different metal oxides is used to modify the film properties since each individual doping element affects the film microstructure in a different way [2].

The aim of the present study is to obtain a detailed understanding of the effect of different additives on the microstructure and also the phase and chemical characteristics of doped SnO<sub>2</sub> thin films. Cu, Fe, Zr and P were chosen as doping elements. These elements increase gas and humidity sensitive properties of SnO<sub>2</sub> thin films, which is important for their practical use.

## 2. Experimental procedures

In order to prepare the spraying solutions a 0.2 M solution of SnCl<sub>4</sub> in ethanol was mixed with the following solutions of the doping elements:

0.2 M ZrCl<sub>4</sub> in ethanol + H<sub>2</sub>O

0.2 M CuCl<sub>2</sub> in ethanol

0.2 M P<sub>2</sub>O<sub>5</sub> in ethanol

0.2 M Fe(NH<sub>4</sub>)(SO<sub>4</sub>)<sub>2</sub> · 12H<sub>2</sub>O in ethanol + H<sub>2</sub>O

0.2 M Fe(C<sub>2</sub>O<sub>4</sub>)<sub>3</sub> in ethanol + H<sub>2</sub>O

0.025 M PdCl<sub>2</sub> in ethanol + H<sub>2</sub>O

The sample codes and corresponding dopant:Sn ratios are listed in Table 1. The solutions were sprayed onto substrates, heated to temperatures of 450–500 °C, at regular time intervals of 10 s. The dis-

tance between the spray nozzle and the substrate was about 50 cm.

The substrates were oxidized silicon wafers and quartz tubes (d = 6 mm, l = 20 mm) or plates.

The thermal treatment of the films was performed in an oxygen atmosphere. In all cases the samples were rapidly cooled to room temperature. The thermal treatment conditions are presented in Table II.

The phase composition of the films was studied by X-ray diffraction (XRD) analysis, using CoK $\alpha$  radiation. The morphology and chemical compositions were investigated by scanning electron microscopy (SEM), energy dispersive X ray spectroscopy (EDX), X ray photoemission (XPS) and Auger electron spectroscopies (AES).

## 3. Results

### 3.1. Phase composition

The XRD data show that in all cases the basic phase in the films is  $\alpha$ -SnO<sub>2</sub> (cassiterite). The investigated doping elements in the SnO<sub>2</sub> films can be classified into two groups:

- the first group: the doping element (Cu, P) does not lead to the appearance of a secondary phase. The peaks of the cassiterite phase remain unshifted.
- the second group: the doping element (Zr, Fe) leads to the appearance of a secondary phase ( $\alpha$ -Fe<sub>2</sub>O<sub>3</sub>-hematite or tetragonal ZrO<sub>2</sub>, respectively).

The XRD analysis of SnO<sub>2</sub>-Fe<sub>2</sub>O<sub>3</sub> films shows that SFC1, SFC2, SFS1 and SFS2 are monophase. The analysis indicates the presence of two phases – cassiterite and hematite for the SFC3–SFC6 and SFS3–SFS6 films. However on the films obtained

TABLE I Composition of the spraying solutions. The different sample codes correspond to the presented dopant:Sn ratios

Samples codes	Initial components	Dopant:Sn ratios
S	SnCl <sub>4</sub>	–
SZ1, SZ2, SZ3, SZ4,	ZrCl <sub>4</sub> , SnCl <sub>4</sub> , PdCl <sub>2</sub>	1:1:0.01, 1:2:0.01, 1:3:0.01, 1:4:0.01
SC1, SC2, SC3, SC4, SC5	CuCl <sub>2</sub> ·2H <sub>2</sub> O, SnCl <sub>4</sub>	1:1, 1:2, 1:3, 1:4, 1:5
SFS1, SFS2, SFS3, SFS4, SFS5, SFS6	Fe(NH <sub>4</sub> )(SO <sub>4</sub> ) <sub>2</sub> ·12H <sub>2</sub> O, SnCl <sub>4</sub>	1:1, 1:4, 1:6, 1:9, 1:19, 4:1
SFC1, SFC2, SFC3, SFC4, SFC5, SFC6	Fe <sub>2</sub> (C <sub>2</sub> O <sub>4</sub> ) <sub>3</sub> , SnCl <sub>4</sub>	1:1, 1:4, 1:6, 1:9, 1:19, 4:1
SP1, SP2, SP3, SP4, SP5	P <sub>2</sub> O <sub>5</sub> , SnCl <sub>4</sub>	1:4, 1:9, 1:19, 1:66, 1:99

TABLE II Conditions of the thermal treatment of the doped SnO<sub>2</sub> films

Film composition	Heating temperature (°C)	Time (min)
SnO <sub>2</sub>	900	30
SnO <sub>2</sub> /CuO	950	30
SnO <sub>2</sub> /ZrO <sub>2</sub>	900	30
SnO <sub>2</sub> /Fe <sub>2</sub> O <sub>3</sub>	900	30
SnO <sub>2</sub> /P <sub>2</sub> O <sub>5</sub>	850	60

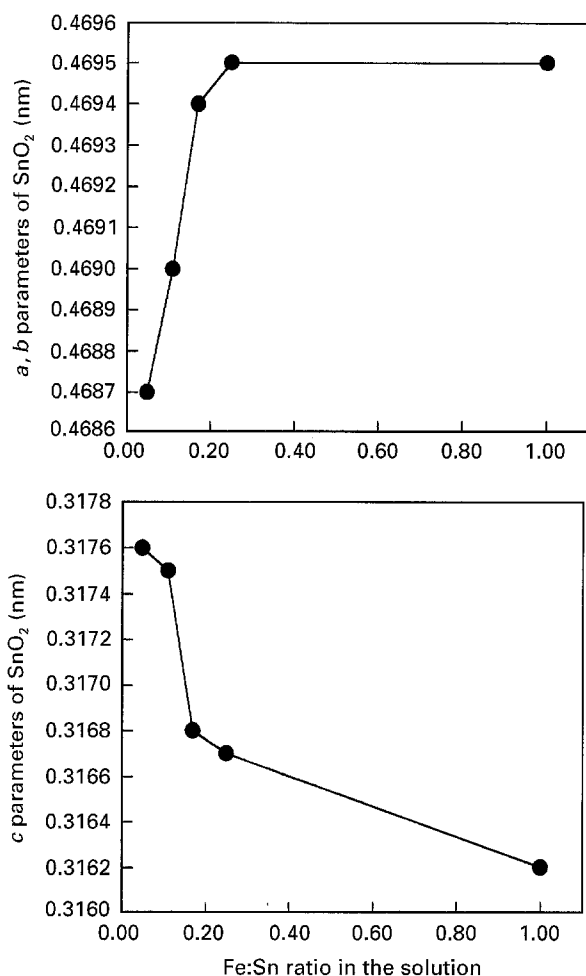


Figure 1 Lattice parameters of SnO<sub>2</sub>-Fe<sub>2</sub>O<sub>3</sub> films as a function of the Fe:Sn ratio in the solution.

from an organic precursor the quantity of hematite is about two times lower than that in the films obtained from Fe(NH<sub>4</sub>)(SO<sub>4</sub>)<sub>2</sub>·12H<sub>2</sub>O. The lattice parameters of doped SnO<sub>2</sub> depend on the iron content – an increase in Fe content leads to increasing values of *a* and *b* and a reduction in the *c* lattice parameters (Fig. 1).

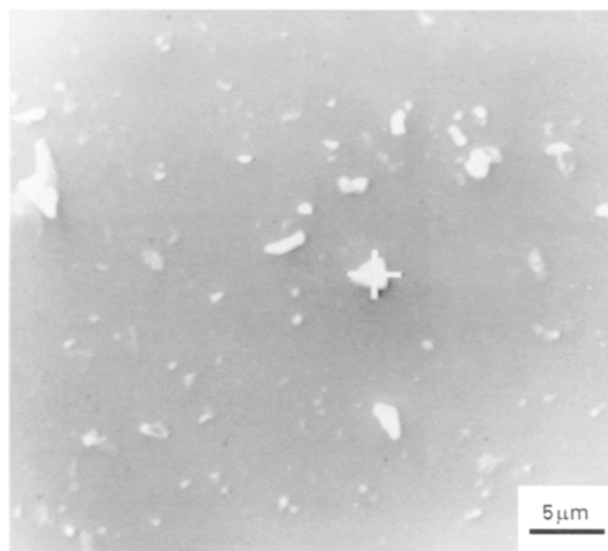


Figure 2 A typical SEM photograph of a sprayed SnO<sub>2</sub> thin film.

On the contrary, the XRD analysis of SnO<sub>2</sub>-ZrO<sub>2</sub>-PdO films reveals that the <1 1 1> peak of the impurity ZrO<sub>2</sub> phase is always present, but that the lattice parameters of doped SnO<sub>2</sub> do not change with the Zr concentration.

### 3.2. Morphology of the doped SnO<sub>2</sub> films

SEM studies of sprayed SnO<sub>2</sub> thin films, reported in the literature [2, 3] reveal that the morphology is characterized by a fine grain matrix with a few large crystallites being located on the surface of the film. Such an arrangement is shown in Fig. 2 for one of the films investigated in this work.

In order to estimate the effect of the dopants on the morphology, pure SnO<sub>2</sub> films were deposited under the same spray conditions and heat treated in an oxygen atmosphere. The average size of the crystallites is 180–200 nm.

The addition of Cu into SnO<sub>2</sub> leads to a decrease in the grain size of about two times. For all the SC1–SC5 films the grain size is around 100 nm (Fig. 3). The Zr also favours the formation of a fine grain structure (Fig. 4(a–c)). The average grain size decreases from 200 to 95 nm for the molar ratios in the films SZ3 and SZ1, respectively.

The doping of SnO<sub>2</sub> films with Fe also causes a decrease in the crystallite size. This influence depends on the nature of the iron salt in the spray solution (Fig. 5(a–d)). The addition of P has a similar effect: the grain size decreases from 90–50 nm (Fig. 6(a–c)).

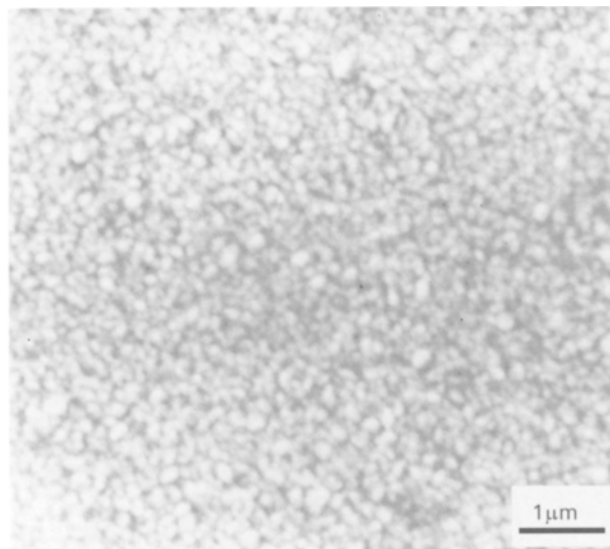


Figure 3 SEM photograph of a  $\text{SnO}_2\text{-CuO}$  thin film obtained from solution with a Cu:Sn ratio = 1:4.

### 3.3. Chemical composition

To study the chemical composition of the films special attention was devoted to the determination of the distribution of the doping elements in the basic layer and in the large crystallites, because such data are missing in the literature. The analysis of the chemical composition of the basic layer was performed in a homogeneous area that did not contain any large crystallites.

In Fig. 7(a–d) the variation of the doping element: Sn ratios in the basic film and in the large crystallites as a function of the corresponding ratios in the spray solution are shown (since the Pd concentration is below the detection limit of EDS analysis no data for this element is presented). Obviously, these variations strongly depend on the type of the introduced element and also on the nature of the dopant salts used. As a general rule, the dopant accumulates mainly in the large crystallites. For dopant:Sn = 1, the dopant concentration in the large crystallites is 3–8 times higher as compared to the basic film.

Another important films characteristic which was examined, is the Sn:O ratio. The AES results show that in all films this ratio is in the range of 1.6–1.8, the value remaining relatively constant with depth into the film. More detailed information has been reported in references [4, 5].

## 4. Discussion

### 4.1. The effect of Cu

The fact that the Cu content in the basic layer is low, explains why the grain size remains unchanged for increased Cu contents in the spray solution. The specific features in the phase and chemical characteristics of  $\text{SnO}_2\text{-CuO}$  films can be explained by reference to the EDS results (Fig. 8a) and XPS data for the SC4 films that reveals that the Cu predominantly accumulates in the large crystallites and in the top 15 nm of the basic film [4]. Due to this, no impurity phase or changes in

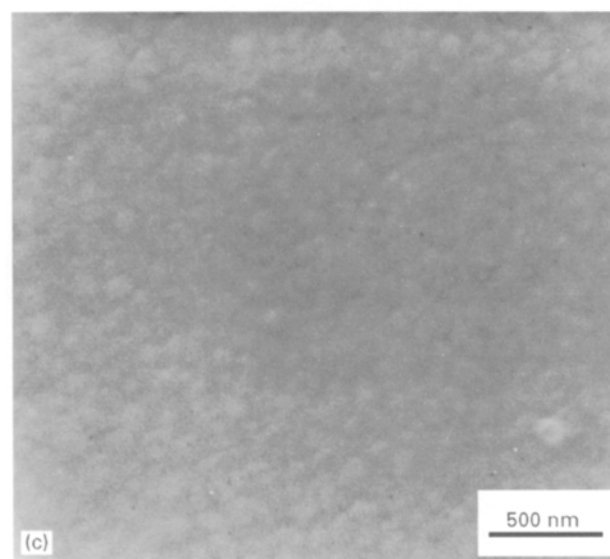
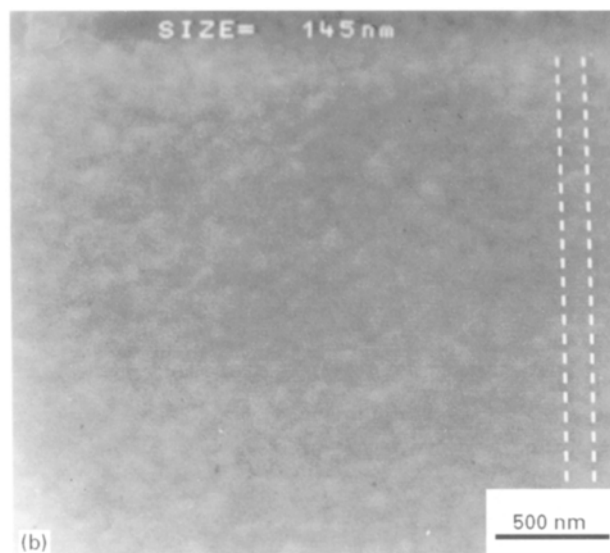
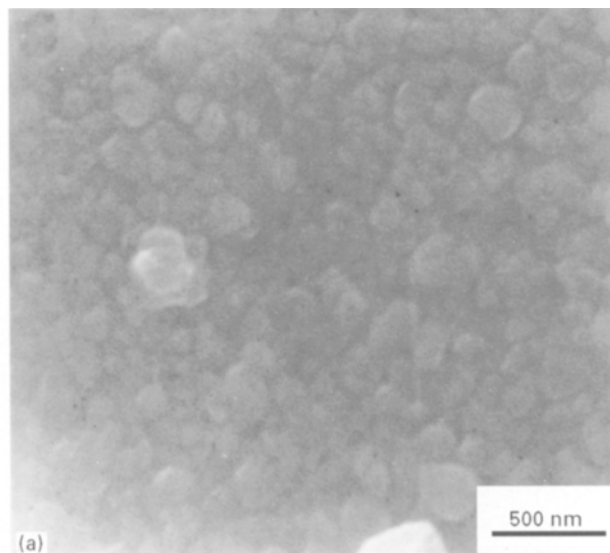


Figure 4 SEM photograph of  $\text{SnO}_2\text{-ZrO}_2\text{-PdO}$  thin films obtained from solutions with Zr:Sn:Pd ratios of (a) 1:3:0.01, (b) 1:2:0.01 and (c) 1:1:0.01.

the lattice parameters of the cassiterite phase are detected.

On the basis of the results described above, it is possible to explain the interaction between the film

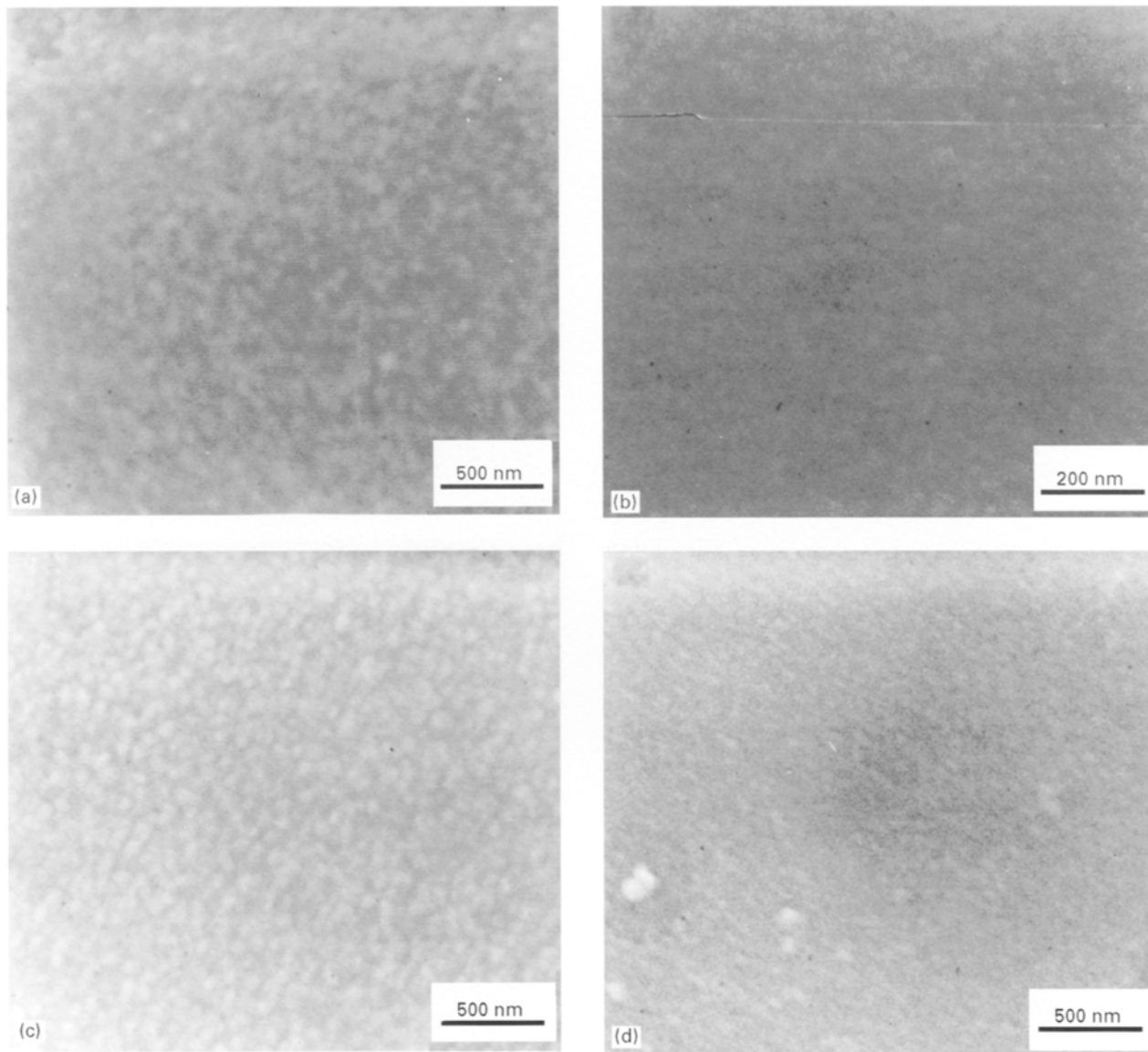


Figure 5 SEM photographs of  $\text{SnO}_2\text{-Fe}_2\text{O}_3$  thin films: – obtained from  $\text{Fe}(\text{NH}_4)(\text{SO}_4)_2 \cdot 12\text{H}_2\text{O}$  with Fe:Sn ratios (a) 1:6 and (b) 1:1 – obtained from  $\text{Fe}_2(\text{C}_2\text{O}_4)_3$  with Fe:Sn ratios of (c) 1:6 and (d) 1:1.

surface and different gases such as  $\text{PH}_3$ ,  $\text{CH}_4$  and also ethanol [4, 6]. Since the Cu is accumulated on the film surface and does not affect the morphology (the grain size and porosity), we can suggest that the Cu by its catalytic influence promotes the gas sensitivity.

#### 4.2. The effect of Zr

In contrast to the  $\text{SnO}_2\text{-CuO}$  films, the introduction of Zr leads to the appearance of a secondary impurity phase (tetragonal  $\text{ZrO}_2$ ) even for low Zr concentrations. This indicates the very low solubility of  $\text{ZrO}_2$  in cassiterite. When the content of Zr increases the dopant precipitates mainly in the form of large crystallites on the film surface. Meanwhile, the concentration of Zr in the basic layer changes very slowly similar to the behaviour observed in the  $\text{SnO}_2\text{-CuO}$  films (Fig. 8b).

It was found that  $\text{SnO}_2\text{-ZrO}_2\text{-PdO}$  films exhibit significant sensitivity to low  $\text{H}_2\text{S}$  and  $\text{PH}_3$  concentrations [3, 7]. The highest sensitivity to  $\text{PH}_3$  is observed for SZ1 films which possess the finest microstructure (Fig. 8b). The decrease in the crystallite size is mainly

due to the addition of  $\text{ZrO}_2$  since the  $\text{SnO}_2$  crystallite growth is only slightly affected by the presence of a small amount of Pd [8]. It is also possible that the increased concentration of  $\text{ZrO}_2$  in the large grains plays an important role in the changes in gas sensitivity. Such an assumption, however, needs to be experimentally verified.

#### 4.3. The effect of Fe

The EDS results reveal that the chemical composition of both the basic layer and the large crystallites is influenced by the nature of the iron salt used. When iron sulphate is used, the Fe predominantly accumulates in the large crystallites; the tendency is more pronounced when the Fe:Sn ratio in the solution increases. The Fe content for films obtained from an organic precursor is similar in both the large crystallites and the basic layer. The SEM observations show that the films obtained from iron oxalate generally possess a finer microstructure in comparison to the SFS films.

It is known that  $\text{SnO}_2\text{-Fe}_2\text{O}_3$  films exhibit a high sensitivity to humidity at room temperature. The humidity sensing properties can be explained by reference to the chemical composition and morphology of the films. When the difference between the chemical

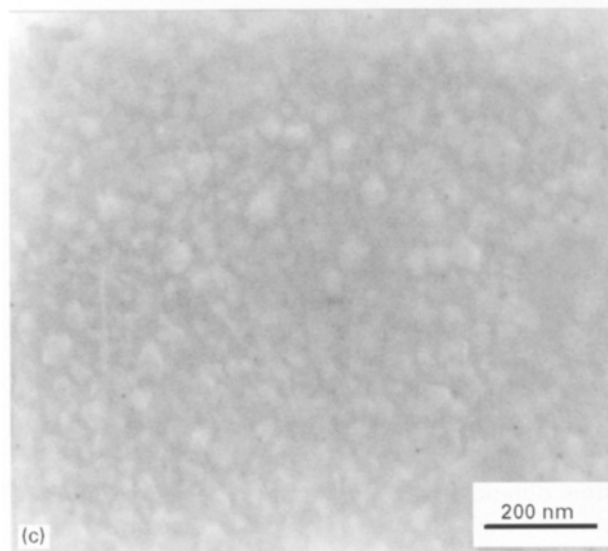
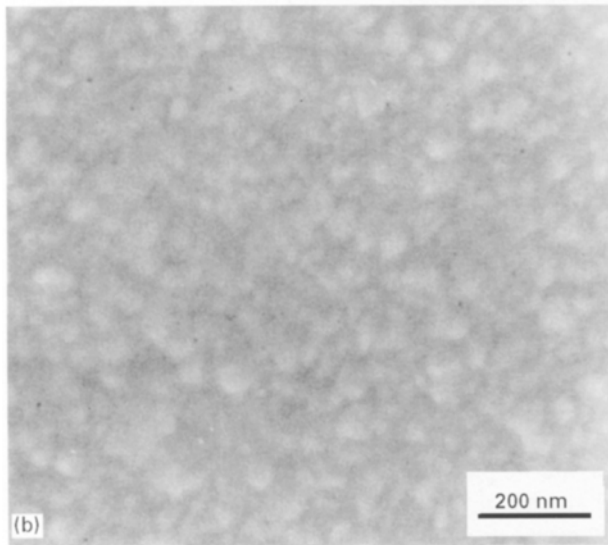
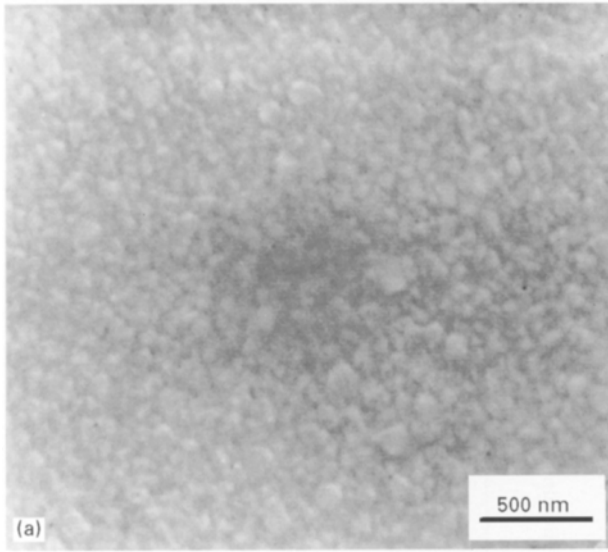


Figure 6 SEM photographs of  $\text{SnO}_2\text{-P}_2\text{O}_5$  thin films obtained from solutions with P:Sn ratios of (a) 1:19 (b) 1:9 and (c) 1:4.

composition of the basic layer and the large crystallites is small, similar chemical reactions and kinetic behaviour can be expected on their surface (Fig. 9). This is observed for the films obtained from  $\text{Fe}_2(\text{C}_2\text{O}_4)_3$  which lead to a linear change of the electrical resistance when the relative humidity increases. When  $\text{Fe}(\text{NH}_4)(\text{SO}_4)_2 \cdot 12\text{H}_2\text{O}$  is used a significant difference in chemical composition (Fig. 9) and a higher quantity of the second phase (hematite) are observed, which is reflected in a more complex electrical behaviour as a function of the relative humidity. The finer microstructure of the SFC films ensures more sites for  $\text{H}_2\text{O}$  adsorption/desorption which in turn determines their shorter response and recovery times in comparison to the SFS films.

#### 4.4. The effect of P

It is known that the elements from group V (Sb for instance) cause a decrease in the resistance of  $\text{SnO}_2$

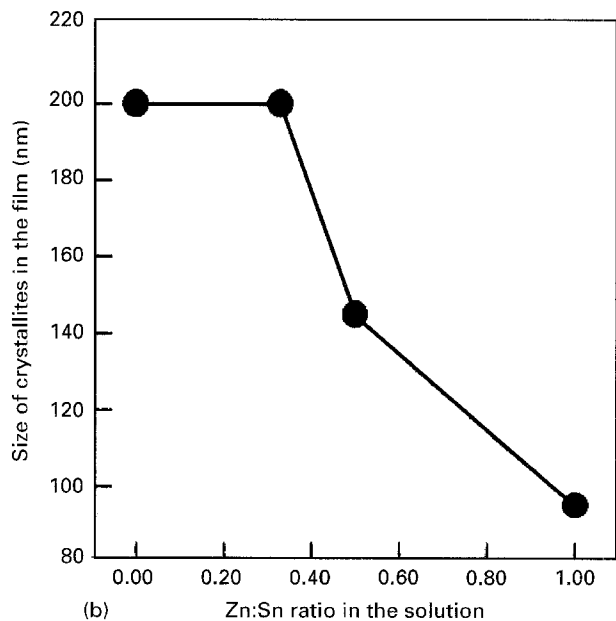
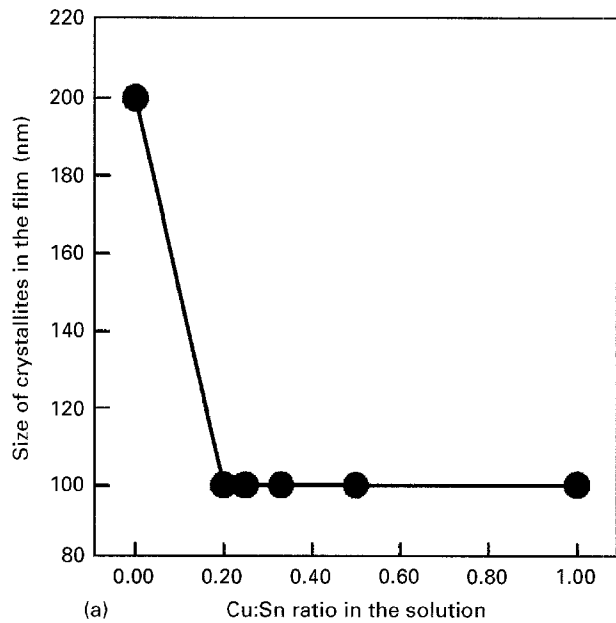


Figure 7 Size of crystallites of the film as a function of the dopant: Sn ratio in the solution.

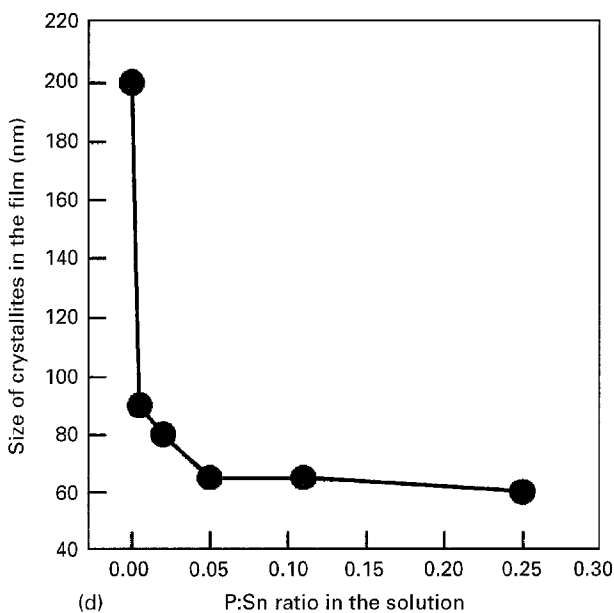
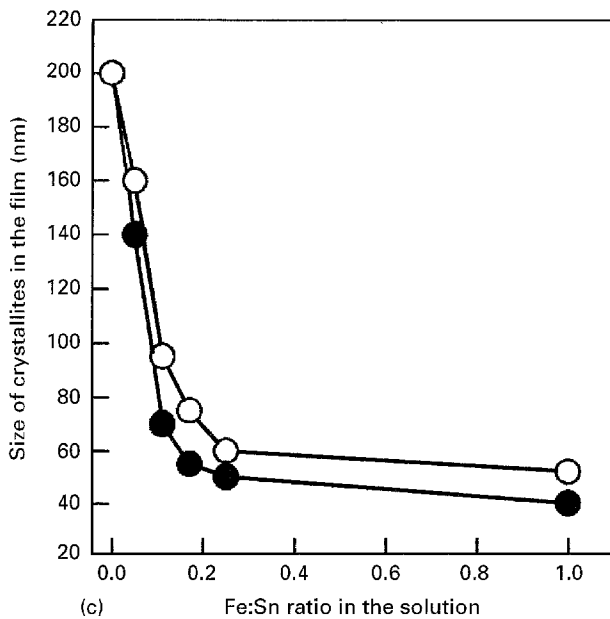


Figure 7 (Continued).

thin films which make them suitable for conducting and photovoltaic materials [2]. In addition to possible application as transparent electrodes [9], they also exhibit interesting gas sensing properties [10].

The aim of adding P to  $\text{SnO}_2$  films is to study its influence on the morphology and the phase composition which as was mentioned previously are important factors that affect the gas sensing properties.

The EDS results reveal that the P content in the basic layer is very low (Fig. 10). In the large crystallites the P:Sn ratio increases up to 0.07, but this ratio is much lower than in the spray solution. The morphology of the films is drastically affected even by small quantities of P (Fig. 6(a-c)). For the films SP3-SP5 the grain size strongly decreases when the P concentration in the spray solution increases. For higher concentrations the change of grain size is much smaller. The dependence shown in Fig. 7d can be explained by the limited solubility of P in the  $\text{SnO}_2$  matrix. In the XRD patterns of the SP3-SP5 films, only peaks of the

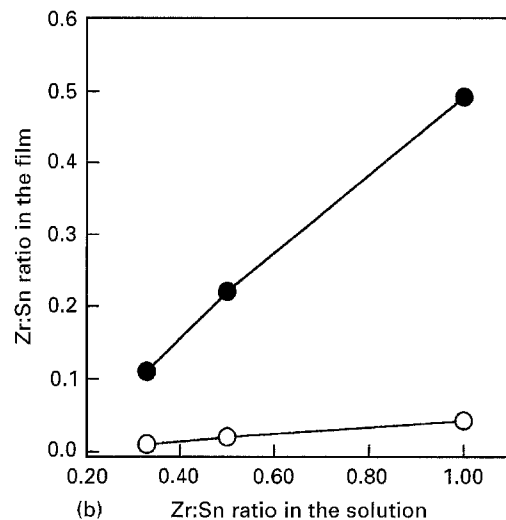
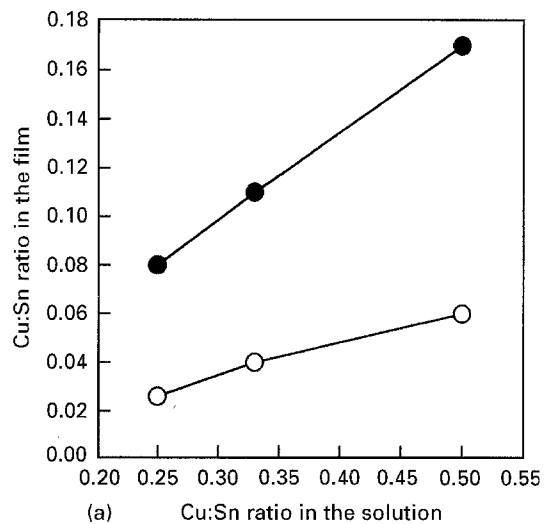


Figure 8 Correlation between (a) Cu:Sn and (b) Zr:Sn ratio in the films and in the solution. The open circles indicate the ratios of the basic layer, the full circles - in the large crystallites.

cassiterite phase are observed, however the crystalline character of the phase decreases when the P content increases. For higher P concentrations, the films SP1 and SP2 are amorphous. These results are similar to results reported for Sb doped  $\text{SnO}_2$  films [4].

The possibility of obtaining  $\text{SnO}_2$  thin films with a fine grain structure by doping with P is a promising way to produce films with potentially good gas sensing properties.

## 5. Conclusions

The morphology and also the chemical and phase composition of sprayed  $\text{SnO}_2$  films doped with Cu, Zr, Fe and P strongly depend on the type and concentration of the doping element. The films obtained from solutions with Cu:Sn ratios of 1:5-1:1, and P:Sn ratios of 1:99-1:19 are single phase cassiterite (the films with higher P content are amorphous). For the films obtained from solutions with Fe:Sn ratios of 1:4-1:1, and for all  $\text{SnO}_2$ - $\text{ZrO}_2$ -PdO films a secondary phase (hematite or tetragonal  $\text{ZrO}_2$ ) appears. As a general rule the film morphology is characterized by a fine grain basic layer and a few large crystallites

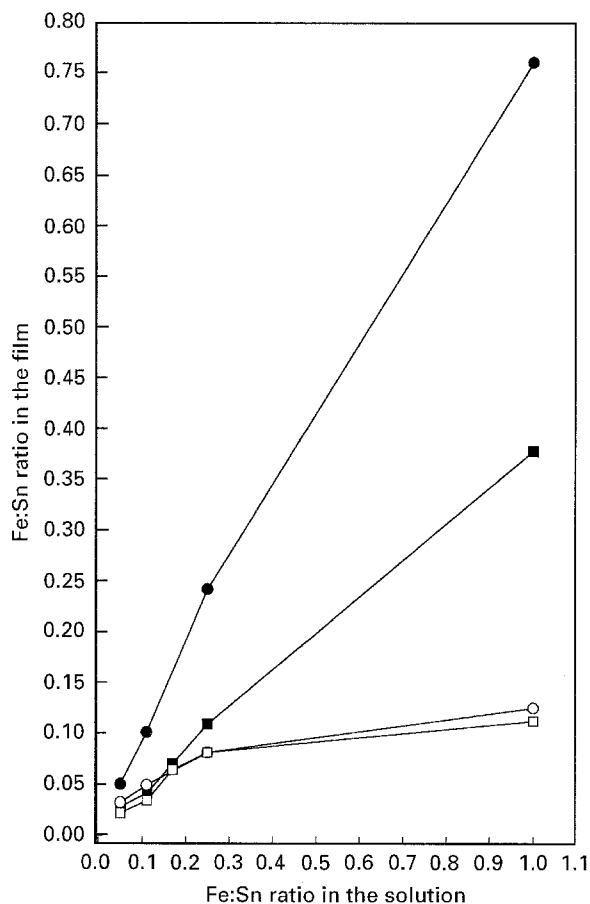


Figure 9 Correlation between the Fe:Sn ratio in the film and in the solution. The circles and squares indicate the results for films obtained from  $\text{Fe}(\text{NH}_4)(\text{SO}_4)_2 \cdot 12\text{H}_2\text{O}$  and  $\text{Fe}_2(\text{C}_2\text{O}_4)_3$ , respectively. The open symbols indicate the ratios in the basic layer, the full symbols – in the large crystallites.

located on the surface. All investigated doping elements lead to a decrease in the grain size of the basic layer. For some of them (Fe, Zr, P) the grain size depends on the doping level in the spray solution. In addition, for the  $\text{SnO}_2\text{-Fe}_2\text{O}_3$  films the nature of the iron salt also affects the grain size. A finer microstructure is obtained using iron oxalate instead of iron sulphate as the initial salt. An increase of the Cu content, however, does not lead to any further decrease in the grain size. The dopant:Sn ratio in the films does not correspond to the one in the spray solution. Furthermore, it was established that the majority of the dopant concentration accumulates in the large crystallites, while only a small quantity is intro-

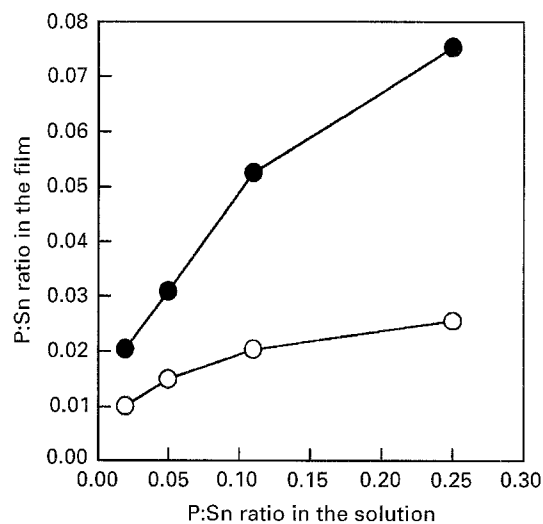


Figure 10 Correlation between the P:Sn ratio in the films and in the solution. The open circles indicate the ratios in the basic layer, the full circles – in the large crystallites.

duced into the basic layer. The distribution of the doping element between the large crystallites and the basic layer in addition to its influence on the grain size are basic factors that determine the gas sensing properties of the doped  $\text{SnO}_2$  films.

## References

1. CHAONAN XU, J. TAMAKI, N. MIURA and N. YAMAZOE, *Sens. Act. B* **3** (1991) 147.
2. A. F. CARROL and L. A. SLACK, *J. Electrochem. Soc.* **123** (1976) 1889.
3. T. RATCHEVA, I. STAMBOLOVA and K. KONSTANTINOV, *Sens. Act. B* **21** (1994) 199.
4. *Idem*, *Thin Solid Films* **217** (1992) 187.
5. T. RACHEVA, I. STAMBOLOVA and T. DONCHEV, *J. Mater. Sci.* **29** (1993) 281.
6. K. NOMURA, Y. UJIHIRA, S. S. SHARMA, A. FUEDA and T. MURAKAMI, *ibid.* **24** (1989) 937.
7. S. KANEFUSA, M. NITTA, M. NARADOME, *IEEE Trans. Elec. Dev.* **ED-35** (1988) 65.
8. M. LABEAU, B. GAUTHERON, J. PENO, M. BALLETRÉGI and J. M. GONZALEZ-CALBET, *Solid State Ionics* **63-65** (1993) 159.
9. B. OREL, U. LAVRENCIC-STANGAR and K. KALCHER, *J. Electrochem. Soc.* **141** (1994) L127.
10. R. G. COOPER, G. N. ADVANI and A. G. JORDAN, *J. Elec. Mater.* **10** (1981) 455.

Received 15 August 1995  
and accepted 13 June 1996